ОПТИЧЕСКИЙ ЖУРНАЛ. 2023. Том 90. № 6. С. 92–99
OPTICHESKII ZHURNAL. 2023. V. 90. № 6. Pp. 92–99

Научная статья
Research Article

Оптический журнал

Оптическое приборостроение и метрология
Optical instrumentation and metrology

DOI: 10.17586/1023-5086-2023-90-06-92-99

Multichannel polarization-selective splitter by semicircle grating scheme

Zhichao Xiong[1], **Bo Wang**[2]✉, **Lichang Li**[3], **Yongchun Zhou**[4], **Guoyu Liang**[5], **Jiaman Hong**[6]

School of Physics and Optoelectronic Engineering, Guangdong University of Technology, Guangzhou, China

[1]2112115109@mail2.gdut.edu.cn https://orcid.org/0000-0002-5084-475X
[2]wangb_wsx@yeah.net https://orcid.org/0000-0002-0927-699X
[3]llchang616@163.com https://orcid.org/0000-0002-7066-9872
[4]yc_z210230@126.com https://orcid.org/0000-0002-8663-2003
[5]liangguoyu2022@163.com https://orcid.org/0000-0002-6131-8851
[6]hongjm2021@163.com https://orcid.org/0000-0003-3309-0316

Abstract

Subject of study. A multilayer semicircle reflective polarization-selective beam splitter is proposed by semicircle grating scheme in this paper. **Purpose of the work.** With the characteristics of polarization selectivity, the beam splitter grating can separate the incident light into three orders (0th order and ±1st orders) for transverse electric polarization and two orders (−1st order and 1st order) for transverse magnetic polarization, respectively. In this work, the proposed splitter achieves the beam polarization selectivity under normal incidence. **Method.** The finite element method is a commonly used analysis method to research micro-nano-optical devices, which can use the mathematical approximation to simulate the real physical system. It is used to calculate the optimal parameters of the proposed polarization-selective beam splitter in this research. **Main results.** By a series of accurate calculations, it is found that the total diffraction efficiencies of transverse electric polarized light can reach 97.27% and transverse magnetic polarization polarized light can reach 96.88% under the optimal grating parameters. It can be found that the grating possesses high efficiency and high reflection optical properties. When the grating parameters such as the grating period and grating thickness fluctuate within a certain range, the impact of the effect of splitting is not big, which means the tolerance is good. **Practical significance.** The polarization-selective splitter by dual-structure scheme has the certain application value for optical fiber communication and laser system.

Keywords: polarization-selective, multichannel beam splitter, semicircle grating, finite element method, grating

Acknowledgment: this work is supported by the Science and Technology Program of Guangzhou (202002030284, 202007010001).

For citation: Zhichao Xiong, Bo Wang, Lichang Li, Yongchun Zhou, Guoyu Liang, Jiaman Hong. Multichannel polarization-selective splitter by semicircle grating scheme (Многоканальный поляризационно-селективный светоделитель по схеме полукруглой решётки) [in English] // Opticheskii Zhurnal. 2023. V. 90. № 6. P. 92–99. http://doi.org/10.17586/1023-5086-2023-90-06-92-99

OCIS codes: 230.1360, 230.5440, 050.1950.

Многоканальный поляризационно-селективный светоделитель по схеме полукруглой решётки

Zhichao Xiong[1], Bo Wang[2]✉, Lichang Li[3], Yongchun Zhou[4], Guoyu Liang[5], Jiaman Hong[6]

School of Physics and Optoelectronic Engineering, Guangdong University of Technology, Guangzhou, China

[1]2112115109@mail2.gdut.edu.cn https://orcid.org/0000-0002-5084-475X
[2]wangb_wsx@yeah.net https://orcid.org/0000-0002-0927-699X
[3]llchang616@163.com https://orcid.org/0000-0002-7066-9872
[4]yc_z210230@126.com https://orcid.org/0000-0002-8663-2003
[5]liangguoyu2022@163.com https://orcid.org/0000-0002-6131-8851
[6]hongjm2021@163.com https://orcid.org/0000-0003-3309-0316

Аннотация

Предмет исследования. Исследование и разработка полукруглого отражающего многослойного поляризационно-селективного светоделителя на основе полукруглой решётки. **Цель работы.** Обеспечение эффективной селективности светоделителя по признаку поляризации пучка. **Метод.** Параметры поляризационно-селективного светоделителя оптимизированы по методу конечных элементов. **Основные результаты.** Эффективность селекции частей разделяемого пучка, отличающихся по видам поляризации, составляет не менее 97,27% для излучения с вектором электрического поля, перпендикулярным плоскости падения (s-поляризация), и 96,88% для излучения поперечной магнитной поляризации поляризованного света (p-поляризации) при малой чувствительности к технологическим отклонениям периода и толщины решётки светоделителя. **Практическая значимость.** Предложенный поляризационно-селективный светоделитель может использоваться для повышения энергетической эффективности волоконно-оптических линий связи и прикладных лазерных систем.

Ключевые слова: селекция по поляризации, многоканальный светоделитель, полукруглая решётка, метод конечных элементов, дифракционная решётка

Благодарность: эта работа проводится при поддержке Научно-технической программы Гуанчжоу (202002030284, 202007010001).

Ссылка для цитирования: Zhichao Xiong, Bo Wang, Lichang Li, Yongchun Zhou, Guoyu Liang, Jiaman Hong. Multichannel polarization-selective splitter by semicircle grating scheme (Многоканальный поляризационно-селективный светоделитель по схеме полукруглой решётки) [на англ. языке] // Оптический журнал. 2023. Т. 90. № 6. С. 92–99. http://doi.org/10.17586/1023-5086-2023-90-06-92-99

Коды OCIS: 230.1360, 230.5440, 050.1950.

INTRODUCTION

The subwavelength grating [1–5] with a simple structure and an excellent performance can be widely used in optical imaging [6–8], polarizer [9], microlens [10], terahertz element [11], liquid crystal cells [12], and laser fields [13–16]. The polarization beam splitter with different diffraction effects can be obtained by rational selection of grating materials and optimization of parameters such as the depth and period of the grating. In this paper, the choice of materials is silver and silicon dioxide. Silver has very good reflection effect. Silicon dioxide is used for the base. The incident wavelength and period of the grating can be controlled to modulate the two beams of polarized light to achieve beam splitting, filtering, and other functions [17–20]. The grating can transmit the energy of transverse electric (TE) polarization light to 0th order, −1st order and 1st order, respectively and transverse magnetic (TM) polarization light to −1st order and 1st order, respectively. In the optical communication under the incident wavelength of 1550 nm, grating possesses a very good polarization-selective splitter effect and high reflectivity.

The research methods of subwavelength gratings mainly include finite element method (FEM) [21], modal method [22], rigorous coupled-wave analysis [23], and finite difference time domain method [24]. The method used in this study is mainly the FEM. The FEM divides the built model into finite, non-overlapping, and connected small units. Within each small unit, the equation is solved using the variational principle, by increasing the number of units and the accuracy of the difference function to improve the approximation of the method. The FEM can also accurately solve the electric field strength of the grating to explain the physical mechanism of the grating.

A semicircle reflex polarization beam splitter is designed in this paper. The grating equation is used in the design of the grating, and the parameters are optimized to ensure satisfying splitting and reflection effects. It is found that the semicircle grating possesses a good reflection performance with simple structure, thus can also be well applicated in the field of optical fiber communications [25–29].

Furthermore, multichannel grating can diffract the TE-polarized light and TM-polarized light into multiple levels. Therefore, this kind of grating has potential application value and is conducive to be applied in the equipment of multi-functional application scene, such as spectrometer [30], wavelength division multiplexing in optical fiber communication [31] and zero elimination stage [32]. The authors in Ref. [32] designed a transmission grating to generate interference pattern by using the characteristics of zeroth-order elimination and used the shear interferometry to measure the terahertz wavefront without reference.

In addition, the reflection grating can couple light to the optical cavity without passing through the substrate. The three-port grating has better coupling effect. A grating with three ports and installed in a second-order Littrow configuration allows even low diffraction efficiency coupling to a high-precision cavity [33]. Moreover, in Ref. [33], the noise of the optical system can also be cancelled out satisfactory. The three-port grating coupler of the second-order Littrow structure is a valuable method to reduce the optical absorption of the cavity coupler substrate in the future gravity wave detectors.

2. THE POLARIZATION-SELECTIVE SPLITTER BY DUAL-STRUCTURE SCHEME

The fabrication process of semicircle grating includes pattern exposure and etching [34–36]. Lithography technology is usually divided into mask technology and maskless technology. Mask technology is divided into contact exposure, proximity exposure and projection exposure. Maskless technology includes electron beam exposure [37], laser direct writing technology [38] and holographic exposure technology [39] and so on. Pattern exposure technology, also known as lithography, is the first link in grating manufacturing. Its quality has an important impact on the grating. Its main process is to transfer the geometric patterns to the photoresist layer coated on the substrate. After the pattern exposure is completed, the pattern on the mask layer needs to be transferred to the required material by physical or chemical methods, which is the etching technology of grating. To begin with, the required grating pattern is transferred to the mask through pattern exposure technology [34, 35]. Then the pattern on the mask is transferred to the designed grating material through two-step etching technology [36]. For the first step, the upper layer is fabricated by the semicircle-etching, which can be based on alternate-tilt method from left to right during etching. For the second step, the lower layer is fabricated by the rectangle-etching. The specific manufacturing process includes glue homogenization, exposure, development, chromium removal, glue removal, etching and chromium removal.

Figure 1 is a three-dimensional schematic diagram of the polarization-selective splitter under normal incidence. The structure of the grating is semicircle and rectangle. The period is d. The λ is the wavelength of the incident light. The radius of semicircle is r. The height of the rectangular shape connection layer is h_1, and the width is $2r$. The height of the silver layer is defined as h_2. The refractive indexes of the silver, SiO_2 and air are $n_3 = 0.469 - i*9.32$, $n_2 = 1.45$, and $n_1 = 1.00$, respectively.

After optimization by the FEM, this semicircle transmission grating with a good beam splitting and reflection effects can be obtained when period $d = 2780$ nm, grating thickness $h_1 = 400$ nm, and $h_2 = 100$ nm. As for the TE polarization, the diffraction efficiency is 97.27%.

As for the TM polarization, the diffraction efficiency is 96.88%. Wang et al. [40] designed a beam splitter which is a surface-relief three-port output with a connecting layer grating under the second Bragg condition, and its efficiency can reach more than 96%. Compared with the beam splitter in this paper, the efficiency of Wang's beam splitter is lower, and the incident angle of their beam splitter is more complex, which causes more difficulties in achieving the high-efficiency output. Therefore, the performance of the beam splitter in this paper is more excellent and has a broader application prospect.

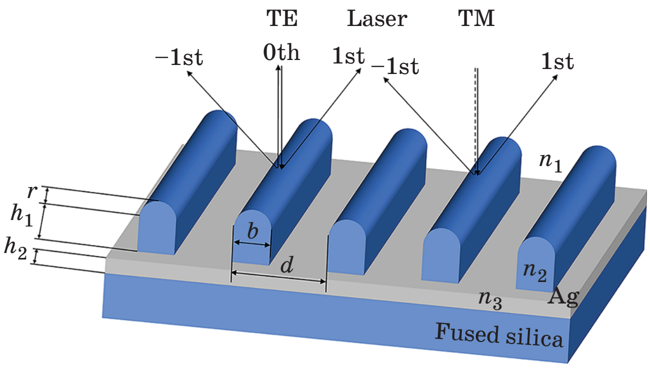

Fig. 1. The diagram of reflective multichannel polarization-selective splitter by semicircle grating scheme

Рис. 1. Схема отражательного многоканального поляризационно-селективного разветвителя по схеме полукруглой решётки

Figure 2 shows the relation between transmission efficiency and period d, duty cycle f under two polarizations. It can be seen from Fig. 2a that when the $f = 0.5$ and the $d = 2780$ nm, the efficiency of 0th order for TE polarization exceeds 40%. When the f ranging from 0.5 to 0.6 and the d increasing from 2780 nm to 2880 nm, the efficiency of which will increase correspondingly. In other domain, the efficiency of which is below 30%. However, it can be seen from Fig. 2b that the efficiency of the 1st order for TE polarization is different from the 0th order. When the f ranging from 0.5 to 0.6 and the d ranging from 2780 nm to 2880 nm, the efficiency will decrease correspondingly. In final picture, when $d = 2680$–2880 nm and $f = 0.4$–0.6, the efficiency of the TM polarization approaches 45%. With a good manufacturing tolerance, the grating is easy to manufacture. From these figures, we can find that the beam splitter in this paper has a wide adjustment range.

Figure 3 presents the normalized electric field of the polarizing beam splitter under normal incidence, which is a good way to explain the physical mechanism of grating. The plane light with a wavelength of 1550 nm incidents from the top of the grating and reflects from the grating layer surface to the air. Fig. 3a and 3b describe the thermoelectric polarization grating beam splitting effects. Due to the periodic grating, the energy distribution is cyclical in the grating, too. Among them, the maximum energy is located in the round, while the energy of the air layer is the lowest.

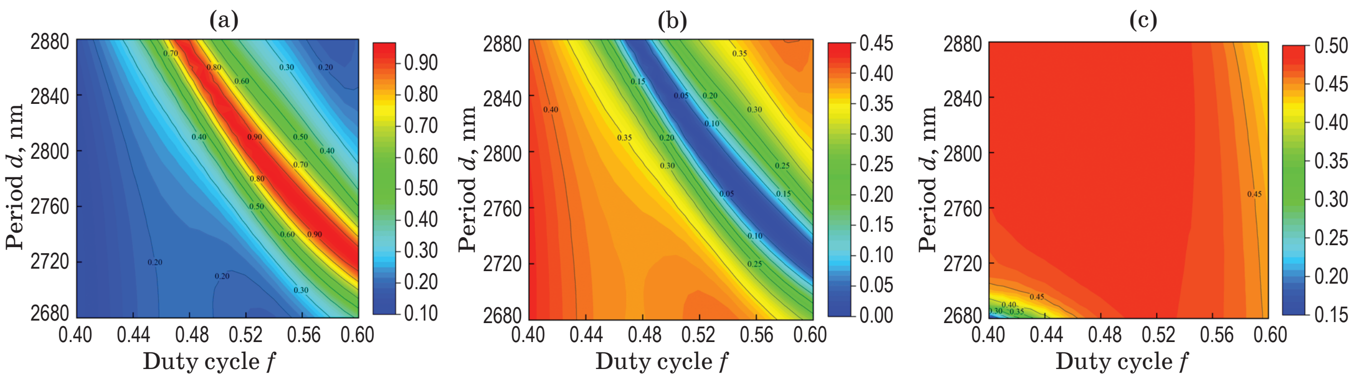

Fig. 2. The relationship of reflection efficiency versus duty cycle f and period d. (a) The efficiency of the 0th order for TE polarization, (b) the efficiency of the 1st order and the −1st order for TE polarization, (c) the efficiency of the 1st order and the −1st order for TM polarization

Рис. 2. Зависимость эффективности отражения от рабочего цикла f и периода d. (a) Эффективность 0-го порядка для s-поляризации, (b) эффективность 1-го порядка и −1-го порядка для s-поляризации, (c) эффективность 1-го порядка и −1-го порядка для p-поляризации

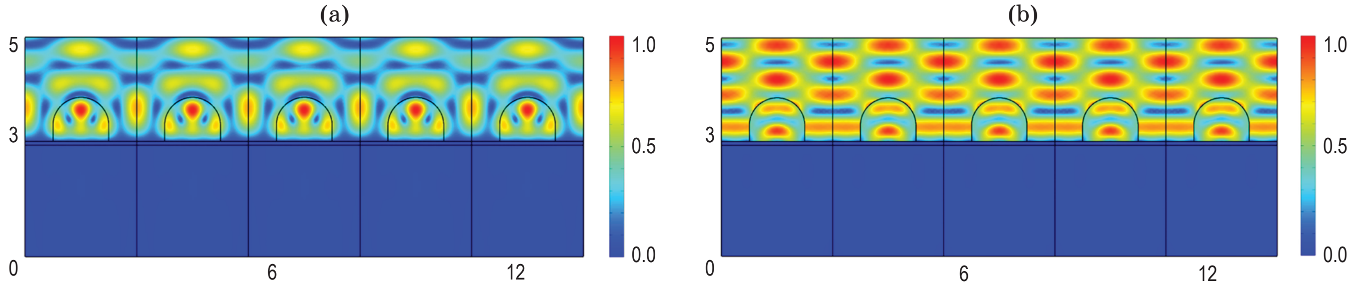

Fig. 3. The normalized electric field of a polarizing beam splitter with wavelength of 1550 nm and period of 2780 nm. (a) TE polarization, (b) TM polarization

Рис. 3. Нормированное электрическое поле поляризационного светоделителя с длиной волны 1550 нм и периодом 2780 нм. (a) s-поляризация, (b) p-поляризация

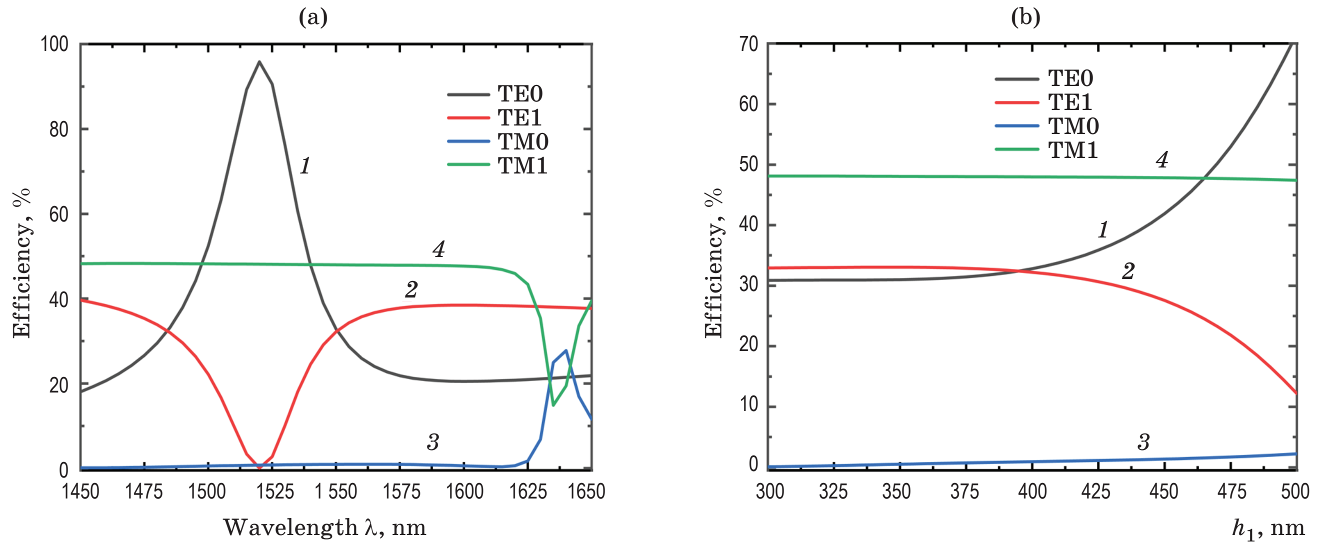

Fig. 4. The effect on the efficiency of each diffraction order (TE 0th (*1*), TE 1st (*2*), TM 0th (*3*), TM 1st (*4*)) by adjusting the incident wavelength λ (a) and the thickness of the rectangle grating ridge h_1 (TE 0th (*1*), TE 1st (*2*), TM 0th (*3*), TM 1st (*4*)) (b)

Рис. 4. Зависимость эффективности дифракционной решётки от длины волны падающего излучения (a) и толщины штрихов её структуры (b) для различных порядков дифракции

3. ANALYSIS AND DISCUSSION

In the actual test and production application [41–44], the thickness of the grating layer and the wavelength of the incident light will have a great influence on the performance of the grating splitter, so it is necessary to analyze the incident wavelength and the thickness of the grating layer. Fig. 4a describes the diffraction efficiency when the wavelength changes. When the wavelength ranging from 1500 nm to 1540 nm, the 0th order polarization has higher efficiency, even more than 90%. Beyond this wavelength range, the 0th order efficiency decreases obviously. When the wavelength exceeds 1540 nm, the efficiency of the 1st order for TE polarization is more than 30%, and the efficiency of the 1st order for TM polarization is more than 45% when the wavelength ranging from 1450 nm to 1625 nm. Fig. 4b describes the relationship between the thickness of the grating layer and diffraction efficiency. When the wavelength locates between 300 nm and 500 nm, the efficiency of the 1st order for TM polarization is 48% with little changes. When the wavelength is ranging from 300 nm to 400 nm, the efficiency of the 0th order for TE polarization remains 32%, and the efficiency of the 1st order for TE polarization is 34%. If it deviates from this range, the efficiency of the 0th order will improve, while that of the 1st order will decrease. In a word, in the certain

The comparison data of incident angle and efficiency in reported Ref. [40] and this paper
Сравнительные данные угла падения и эффективности, указанные в статье [40] и в этой статье

	TE polarization	TM polarization	Type of incident angle
Surface-relief beam splitter [40]	No more 96.50%	No more 96.20%	Second Bragg incidence
Semicircle reflection beam splitter	At least 97.27%	At least 96.88%	Normal incidence

range, the wider the incident wavelength range, the smaller grating layer thickness, the better performance of the beam splitter. The data show that the performance of this polarization-selective splitter is obviously better than the grating proposed in Ref. [40], and the detailed parameter comparison is listed in Table.

4. CONCLUSION

In this paper, a semicircle multi-channel polarization-selective splitting grating is described under normal incidence. Semicircle grating has the property of polarization selection in this article. Under the TE polarization, the efficiency of the 0th order, -1st order and 1st order is more than 32%. Under the TM polarization, the efficiency of -1st order and 1st order is nearly 48%, while the efficiency of the 0th order is nearly 1%. Both the efficiencies of the two polarizations are more than 96%.

Through the FEM, the polarization-selective beam splitter parameters are optimized. The results show that the grating has a stable and efficient reflection output efficiency and good selectivity in a certain optical communication band and a certain grating layer thickness range. At the same time, the novel scheme of the polarization-selective splitter for optical fiber communication and laser system also has the certain research and application value.

REFERENCES

1. Li H., Wang K., Qian L. Tunable color filter with non-subwavelength grating at oblique incidence // Optik. 2020. V. 207. P. 164432. http://doi.org/10.1016/j.ijleo.2020.164432
2. He W., Zhao J., Dong M., Meng F., Zhu L. Wavelength-switchable erbium-doped fiber laser incorporating fiber Bragg grating array fabricated by infrared femtosecond laser inscription // Opt. Laser Technol. 2019. V. 127. P. 106026. http://doi.org/10.1016/j.optlastec.2019.106026
3. Li C., Zhang M., Bowers J., Dai D. Ultra-broadband polarization beam splitter with silicon subwavelength-grating waveguides // Opt. Lett. 2020. V. 45. № 8. P. 2259–2262. http://doi.org/10.1364/OL.389207
4. Wang B., Ren L., Kong X., Xu Y., Ren K., Yang W., Cheng S., Chen F., Song F. Study on fabrication, spectrum and torsion sensing characteristics of microtapered long-period fiber gratings // Optik. 2020. V. 207. P. 164445. http://doi.org/10.1016/j.ijleo.2020.164445
5. Lee H-S., Kwak J., Seong T.Y., Hwang G., Kim W., Kim I., Lee K. Optimization of tunable guided-mode resonance filter based on refractive index modulation of graphene // Sci. Rep. 2019. V. 9. P. 19951. http://doi.org/10.1038/s41598-019-56194-4
6. Wolbromsky L., Dudaie M., Shinar S., Shaked N. Multiplane imaging with extended field-of-view using a quadratically distorted grating // Opt. Commun. 2020. V. 463. P. 125399. http://doi.org/10.1016/j.optcom.2020.125399
7. Yoo H., Jang J.U., Jang J.Y. Analysis of imaging characteristics of parallax images in double diffraction grating imaging // Optik 2019. V. 207. P. 163826. http://doi.org/10.1016/j.ijleo.2019.163826
8. Sanjuan F., Gaborit G., Coutaz J.L. Sub-wavelength terahertz imaging through optical rectification // Sci. Rep. 2018. V. 8. P. 13492. https://doi.org/10.1038/s41598-018-31970-w
9. Zhang J., Yang J., Liang L., Wu W. Broadband TM-mode-pass polarizer and polarization beam splitter using asymmetrical directional couplers based on silicon subwavelength grating // Opt. Commun. 2017. V. 407. P. 46–50. http://doi.org/10.1016/j.optcom.2017.08.044
10. Li D., Wang X., Ling J., Yuan Y. Multiwave length achromatic microlens through phase compensation based on the subwavelength metallic nanostructures // Opt. Commun. 2019. V. 445. P. 90–95. http://doi.org/10.1016/j.optcom.2019.04.029
11. Fang B., Chen L., Jing X. Electromagnetic dipole resonant characteristics of all dielectric one dimensional grating in terahertz region // Optik. 2018. V. 171. P. 130–138. http://doi.org/10.1016/j.ijleo.2018.06.038
12. Sasaki T., Kushida H., Sakamoto M., Noda K., Okamoto H., Kawatsuki N., Ono H. Liquid crystal cells with subwavelength metallic gratings for transmissive terahertz elements with electrical tunability // Opt. Commun. 2018. V. 431. P. 63–67. http://doi.org/10.1016/j.optcom.2018.09.013
13. Chen Z., Li Y., Zhang Y., Hu C., Sun X. Preparation of miRNA137 biomimetic coated coronary stent by dual-injection four-beam laser interference // Optik. 2020. V. 207. P. 164315. http://doi.org/10.1016/j.ijleo.2020.164315
14. Wang H., Zhao F., Yan Z., Hong X., Song J., Zhou K., Zhang T., Zhang W., Wang Y. All-fiber polarization interference filter based uniform multiwave length erbium-doped fiber laser // Laser Phys. 2019. V. 29. № 5. P. 055105. http://doi.org/10.1088/1555-6611/ab0d0e

15. Yang N., Xiao J. A compact silicon-based polarization independent power splitter using a three-guide directional coupler with subwavelength gratings // Opt. Commun. 2019. V. 459. P. 125095. http://doi.org/10.1016/j.optcom.2019.125095
16. Wu H., Lu J., Huang L., Zeng X., Zhou P. All-fiber laser with agile mode-switching capability through intracavity conversion // IEEE Photon. J. 2019. V. 12. № 2. P. 1500709. http://doi.org/10.1109/JPHOT.2019.2911270
17. Liang X., Zhang X., Chen Y., Zhang Y. Experiment demonstration of DFB semiconductor laser array based on s-bent waveguide with sampled grating // Optik. 2019. V. 202. P. 163557. http://doi.org/10.1016/j.ijleo.2019.163557
18. Hu J., Xing Z., Zou M., Liu B., Guo X., Fang F., Sun Y., Sun Q., Yan Z., Zhou K., Liu D., Zhang L. In-fiber dispersion compensated polarizer and mode-locked fiber laser application // IEEE Photon. Technol. Lett. 2020. V. 32. № 9. P. 510–513. http://doi.org/10.1109/LPT.2020.2981170
19. Yang W., Yu X., Zhang J., Deng X. Plasmonic transmitted optical differentiator based on the subwavelength gold gratings // Opt. Lett. 2020. V. 45. № 8. P. 2295–2298. http://doi.org/10.1364/OL.390566
20. Liu X., Wang C., Xu Y., Leng Y., Li R. A broadband low-chromatic-aberration single grating Offner stretcher by 3D analysis // Opt. Commun. 2020. V. 465. P. 125502. http://doi.org/10.1016/j.optcom.2020.125502
21. Zeng L., Chen M., Chen W., Yan W., Li Z., Yang F. Si-grating-assisted SPR sensor with high figure of merit based on Fabry–Perot cavity // Opt. Commun. 2019. V. 457. P. 124641. http://doi.org/10.1016/j.optcom.2019.124641
22. Gong B., Wen H., Li H. Polarization-independent two-layer grating with five-port splitting output under normal incidence // IEEE Photon. J. 2020. V. 12. № 2. P. 6500208. http://doi.org/10.1109/JPHOT.2020.2978882
23. Gaylord T.K., Moharam M.G., Pommet D.A., Grann E.B. Stable implementation of the rigorous coupled-wave analysis for surface-relief gratings: enhanced transmittance matrix approach // J. Opt. Soc. Am. A. 1995. V. 12. № 5. P. 1077–1086. http://doi.org/10.1364/JOSAA.12.001077
24. Xu Y., Wang F., Gao Y., Chen W., Chen C., Wang X., Yi Y., Sun X., Zhang D. Efficient polymer waveguide grating coupler with directionality enhancement // Opt. Commun. 2020. V. 463. P. 125418. http://doi.org/10.1016/j.optcom.2020.125418
25. Zhang R., Peng P., Li X., Liu S., Zhou Q., He J., Chen Y., Shen S., Yao S., Chang G. 4x100-Gb/s PAM-4 FSO transmission based on polarization modulation and direct detection // IEEE Photon. Technol. Lett. 2019. V. 31. № 10. P. 755–758. http://doi.org/10.1109/LPT.2019.2906753
26. Lou J., Cheng T., Li S. Ultra-short polarization beam splitter with square lattice and gold film based on dual-core photonic crystal fiber // Optik 2018. V. 179. P. 128–134. http://doi.org/10.1016/j.ijleo.2018.10.109
27. Reyes-Vera E., Usuga-Restrepo J., Jimenez-Durango C., Montoya-Cardona J., Gomez-Cardona N. Design of low-loss and highly birefringent porous-core photonic crystal fiber and its application to terahertz polarization beam splitter // IEEE Photon. J. 2018. V. 10. № 4. P. 5900413. http://doi.org/10.1109/JPHOT.2018.2860251
28. Lee S.-L., Kim J., Choi S., Kim M., Kim D., Lee Y. Polarization-diversified-loop-based optical fiber interleaving filter with polarization-controlled free spectral range // Opt. Commun. 2020. V. 463. P. 125345. http://doi.org/10.1016/j.optcom.2020.125345
29. Zhang B., Chen W., Wang P., Dai S., Jiang W., Liang W., Lu H., Ding J., Li J., Li Y., Fu Q., Dai T., Yu H., Yang J. Switchable polarization beam splitter based on GST-on-silicon waveguides // IEEE Photon. J. 2020. V. 12. № 2. P. 6600610. http://doi.org/10.1109/JPHOT.2020.2977979
30. Sun L.-X. Simultaneous quantitative analysis of multi-elements in alloy samples by laser-induced breakdown spectroscopy // Spectrosc. Spectr. Anal. 2009. V. 29. № 12. P. 3375–3378. http://doi.org/10.3964/j.issn.1000-0593(2009)12-3375-04
31. Li B., Du B.-Z., Zhu J.-P. Study on planar concave diffraction grating with Bragg reflector facets // Acta Phys. Sin. 2015. V. 64. № 15. P. 154211. http://doi.org/10.7498/aps.64.154211
32. Agour M., Fallorf C., Taleb F., Castro-Camus E., Koch M., Bergmann R.B. Terahertz reference less wave front sensing by means of computational shear-interferometry // Opt. Express. 2022. V. 30. № 5. P. 7068–7081. http://doi.org/10.1364/OE.450708
33. Meinders M., Kroker S., Singh A.P., Kley E.B., Tunnermann A., Danzmann K., Schnabel R. Cancellation of lateral displacement noise of three-port gratings for coupling light to cavities // Opt. Lett. 2015. V. 40. № 9. P. 2053–2055. http://doi.org/10.1364/OL.40.002053
34. Wang J., Zhou C., Ma J., Zong Y., Jia W. Highly efficient reflective Dammann grating with a triangular structure // Appl. Opt. 2016. V. 55. № 19. P. 5203–5207. http://doi.org/10.1364/AO.55.005203
35. Wang J., Zhou C., Ma J., Zong Y., Jia W. Modal analysis of 1×3 reflective triangular gratings under normal incidence // Chin. Opt. Lett. 2017. V. 15. № 4. P. 040902. http://doi.org/10.3788/COL201715.040902
36. Cao H., Wu J., Yu J., Ma J. High-efficiency polarization-independent wideband multilayer dielectric reflective bullet-alike cross-section fused-silica beam combining grating // Appl. Opt. 2018. V. 57. № 4. P. 900. http://doi.org/10.1364/AO.57.000900
37. Liu S., Zhou F., Jin A., Yang H., Ma Y., Li H., Gu C., Lu L., Jiang B., Zheng Q., Wang S., Peng L. Fabrication of graphite nanostructures // Acta Phys. Sin. 2005. V. 54. № 9. P. 4251–4255. http://doi.org/10.7498/aps.54.4251
38. Cui B., Yang Y.-P., Ma P., Yang X.-Y., Ma L.-W. Optical modulation characteristics of all-dielectric grating at terahertz frequencies // Acta Phys. Sin. 2016. V. 65. № 7. P. 074209. http://doi.org/10.7498/aps.65.074209
39. Li H., Yang C.-A., Xie S.-W., Huang S.-S., Chai X.-L., Zhang Y., Wagn J.-L., Niu Z.-C. Laterally-coupled distributed feedback lasers with optimized gratings by holographic lithography etching // J. Infrared Millim. Waves. 2018. V. 37. № 2. P. 140–144. http://doi.org/10.11972/j.issn.1001-9014.2018.02.003
40. Wang B., Zhu W., Li H., Yin S., Su C., Chen L., Lei L., Zhou J. Surface-relief three-port output with a connecting layer grating under the second Bragg condition // Surf. Rev. Lett. 2019. V. 26. № 2. P. 1850140. http://doi.org/10.1142/S0218625X18501408
41. Kaur G., Kaler R. Wavelength remodulation and dispersion compensation for full-duplex radio over fiber system using fiber Bragg grating // Optik. 2019. V. 206. P. 163223. http://doi.org/10.1016/j.ijleo.2019.163223

42. Wang T. Electromagnetic field quantization and quantum optical input-output relation for grating // Sci. Rep. 2019. V. 9. P. 19992. http://doi.org/10.1038/s41598-019-56197-1
43. Hao A., Han Q., Hui Z., He F., Wang Z., Chen D. Imaging analysis of holographic concave grating spectrometer // Optik. 2020. V. 204. P. 164193. http://doi.org/10.1016/j.ijleo.2020.164193
44. Dong D., Liu Y., Fei Y., Fan Y., Li J., Fu Y. Polarization beam splitter based on extremely anisotropic black phosphorus ribbons // Opt. Express. 2020. V. 28. № 6. P. 8371–8383. http://doi.org/10.1364/OE.388845

AUTHORS

Zhichao Xiong — Student, Guangdong University of Technology, 510006, Guangzhou, China; http://orcid.org/0000-0002-5084-475X, 2112115109@mail2.gdut.edu.cn

Bo Wang — Doctor of Optical Engineering, Professor, Guangdong University of Technology, 510006, Guangzhou, China; http://orcid.org/0000-0002-0927-699X, wangb_wsx@yeah.net

Lichang Li — Student, Guangdong University of Technology, 510006, Guangzhou, China; http://orcid.org/0000-0002-7066-9872, llchang616@163.com

Yongchun Zhou — Student, Guangdong University of Technology, 510006, Guangzhou, China, http://orcid.org/0000-0002-8663-2003, yc_z210230@126.com

Guoyu Liang — Student, Guangdong University of Technology, 510006, Guangzhou, China, http://orcid.org/0000-0002-6131-8851, liangguoyu2022@163.com

Jiaman Hong — Student, Guangdong University of Technology, 510006, Guangzhou, China, http://orcid.org/0000-0003-3309-0316, hongjm2021@163.com

The article was submitted to the editorial office 14.10.2021
Approved after review 01.03.2023
Accepted for publication 27.04.2023

Статья поступила в редакцию 14.10.2021
Одобрена после рецензирования 01.03.2023
Принята к печати 27.04.2023